THE JOURNAL OF BIOLOGICAL CHEMISTRY VOL. 288, NO. 35, pp. 25129–25142, August 30, 2013
© 2013 by The American Society for Biochemistry and Molecular Biology, Inc. Published in the U.S.A.

Macromolecular Composition Dictates Receptor and G Protein Selectivity of Regulator of G Protein Signaling (RGS) 7 and 9-2 Protein Complexes in Living Cells*

Received for publication, February 15, 2013, and in revised form, July 8, 2013 Published, JBC Papers in Press, July 15, 2013, DOI 10.1074/jbc.M113.462283

Ikuo Masuho, Keqiang Xie, and Kirill A. Martemyanov[1]

From the Department of Neuroscience, The Scripps Research Institute Florida, Jupiter, Florida 33410

Background: RGS7 and RGS9-2 regulate G protein signaling in the striatum, but the selectivity of their action is largely unknown.
Results: RGS protein complexes show distinct patterns of receptor and G protein selectivity.
Conclusion: Macromolecular composition dictates receptor and G protein selectivity of the RGS7 and RGS9-2 protein complexes.
Significance: These data demonstrate novel mechanisms contributing to the regulation of striatal G protein signaling.

Regulator of G protein signaling (RGS) proteins play essential roles in the regulation of signaling via G protein-coupled receptors (GPCRs). With hundreds of GPCRs and dozens of G proteins, it is important to understand how RGS regulates selective GPCR-G protein signaling. In neurons of the striatum, two RGS proteins, RGS7 and RGS9-2, regulate signaling by μ-opioid receptor (MOR) and dopamine D2 receptor (D2R) and are implicated in drug addiction, movement disorders, and nociception. Both proteins form trimeric complexes with the atypical G protein β subunit Gβ5 and a membrane anchor, R7BP. In this study, we examined GTPase-accelerating protein (GAP) activity as well as Gα and GPCR selectivity of RGS7 and RGS9-2 complexes in live cells using a bioluminescence resonance energy transfer-based assay that monitors dissociation of G protein subunits. We showed that RGS9-2/Gβ5 regulated both Gi and Go with a bias toward Go, but RGS7/Gβ5 could serve as a GAP only for Go. Interestingly, R7BP enhanced GAP activity of RGS7 and RGS9-2 toward Go and Gi and enabled RGS7 to regulate Gi signaling. Neither RGS7 nor RGS9-2 had any activity toward Gz, Gs, or Gq in the absence or presence of R7BP. We also observed no effect of GPCRs (MOR and D2R) on the G protein bias of R7 RGS proteins. However, the GAP activity of RGS9-2 showed a strong receptor preference for D2R over MOR. Finally, RGS7 displayed an four times greater GAP activity relative to RGS9-2. These findings illustrate the principles involved in establishing G protein and GPCR selectivity of striatal RGS proteins.

Signal transduction through G protein-coupled receptors (GPCRs)[2] regulates fundamental processes in the nervous system, including neuronal excitability and neurotransmitter release (1). GPCRs activate heterotrimeric G proteins, which in turn engage a wide range of the intracellular effectors to produce a cellular response. Activation of G proteins entails their binding to GTP and resulting dissociation into Gα-GTP and G$\beta\gamma$ subunits. The extent and duration of signaling in GPCR pathways is critically controlled by the regulator of G protein signaling (RGS) proteins that limit G protein activity (2, 3). RGS proteins bind directly to activated Gα and facilitate the GTP hydrolysis, thus serving as GTPase-accelerating proteins (GAPs).

In humans, 17 Gα, about 865 GPCR, and ~30 RGS genes have been identified (4–6). With most of the components expressed in the nervous system, this forms a formidable array of possible combinations. However, activation of individual GPCR pathways often produces unique cellular and behavioral responses. Understanding the mechanisms of this signaling selectivity is one of the biggest challenges in studying neuronal GPCR pathways.

Neurons of the striatum, a nucleus that plays a major role in reward behavior and motor control, express a number of GPCRs that respond to many neurotransmitters, including dopamine, opioids, serotonin, and acetylcholine (7, 8). Several studies have demonstrated that the long splice isoform of RGS9 (RGS9-2) serves as a critical GAP in these neurons (9, 10). In particular, RGS9-2 has been shown to regulate signaling downstream from D2 dopamine (D2R) and μ-opioid (MOR) receptors and has been implicated in drug addiction and movement disorders (11–15). However, no studies directly examined the impact of RGS9-2 on G protein dynamics activated by D2R and MOR.

Recent behavioral studies implicated another RGS protein in the striatum, RGS7, in controlling the effects of addictive drugs and suggested that it may be differentially involved in controlling MOR and D2R signaling (16). Both RGS9-2 and RGS7 share extensive homology in their macromolecular organization. In addition to the catalytic RGS domain, they possess the N-terminal Dishevelled, EGL-10, Pleckstrin/Dishevelled, EGL-10, Pleckstrin helical extension module and a G protein γ sub-

* This work was supported, in whole or in part, by National Institutes of Health Grants DA021743 and DA026405.
[1] To whom correspondence should be addressed: Department of Neuroscience, The Scripps Research Institute Florida, 130 Scripps Way, Jupiter, FL 33458. Tel.: 561-228-2770; Fax: 561-228-2775; E-mail: kirill@scripps.edu.
[2] The abbreviations used are: GPCR, G protein-coupled receptor; RGS, regulator of G protein signaling; GAP, GTPase-activating protein; D2R, D2 dopamine receptor; MOR, μ-opioid receptor; BRET, bioluminescence resonance energy transfer; CRE, cAMP response element; AC, adenylyl cyclase.

unit-like domain (10). The G protein γ subunit-like domain forms a constitutive complex with the atypical G protein β subunit, Gβ5 (17, 18), and both RGS7 and RGS9-2 exist as obligatory dimers with Gβ5 (19). In the striatum, RGS/Gβ5 dimers associate with membrane anchor R7BP (20) that recruits them to the plasma membrane and potentiates the GAP activity (21, 22). What remains completely unexplored is the relative activity and selectivity of the RGS7 and RGS9-2 complexes, as well as the role of R7BP in this process.

In this study, we examined the ability of the RGS7/Gβ5 and RGS9-2/Gβ5 complexes to regulate G protein signaling by MOR and D2R under the native environment of living cells using a bioluminescence resonance energy transfer (BRET)-based assay. We report a marked differences in the catalytic activity of complexes as well as their G protein and GPCR selectivity, depending on their macromolecular composition. Our findings illustrate mechanisms for establishing the selective regulation of striatal GPCR signaling pathways.

EXPERIMENTAL PROCEDURES

DNA Constructs, Antibodies, and Recombinant Proteins—Construction of RGS9-2, Gβ5S, and R7BP in pcDNA3.1 was described previously (20). RGS7, Gβ1, Gγ2, and Gαz in pcDNA3.1+ were purchased from the Missouri S&T cDNA Resource Center. Generation of sheep anti-RGS9-2 (20) and rabbit anti-RGS7 (23) were described previously. Rabbit anti-Gβ5 and rabbit anti-R7BP were gifts from Dr. William Simonds (NIDDK, National Institutes of Health, Bethesda, MD). Mouse anti-β-actin (AC-15) (Sigma-Aldrich), rabbit anti-Gαo (K-20) (Santa Cruz Biotechnology), rabbit anti-Gαi1/2 (Affinity BioReagents), rabbit anti-D2R (H-50) (Santa Cruz Biotechnology), mouse anti-GFP (clones 7.1 and 13.1) (Roche Applied Science) and rabbit anti-*Renilla* luciferase (GeneTex) were purchased. Recombinant His-tagged RGS7 and RGS9-2 were coexpressed with Gβ5S in Sf9 insect cells, and the complexes were purified as described previously (24).

Cell Culture and Transfection—HEK293T/17 cells were grown in DMEM supplemented with 10% FBS, minimum Eagle's medium non-essential amino acids, 1 mM sodium pyruvate, and antibiotics (100 units/ml penicillin and 100 μg/ml streptomycin) at 37 °C in a humidified incubator containing 5% CO_2. For transfection, cells were seeded into 6-cm dishes at a density of 4×10^6 cells/dish. After 4 h, expression constructs (total 5 μg/dish) were transfected into the cells using PLUS (5 μl/dish) and Lipofectamine LTX (8 μl/dish) reagents. The GPCR (μ-opioid receptor or dopamine D2 receptor), Gα (Gαo, Gαi1, Gαz, Gαq, or Gαs), Venus 156-239-Gβ, Venus 1–155-Gγ2, masGRK3ct-Rluc8, Gβ5S, and R7BP constructs were transfected at a 1:2:1:1:1:1:1 ratio with different amounts of R7 RGS (RGS7 or RGS9-2). An empty vector was used to normalize the amount of transfected DNA.

Fast Kinetic BRET Assay—Agonist-dependent cellular measurements of BRET between masGRK3ct-Rluc8 and Gβ1γ2-Venus were performed to visualize the action of G protein signaling in living cells, as described previously, with slight modifications (25). 16 to 24 h post-transfection, HEK293T/17 cells were washed once with PBS containing 5 mM EDTA (EDTA/PBS) and detached by incubation in EDTA/PBS at room temperature for 10 min. Cells were harvested with centrifugation at 500 g for 5 min and resuspended in PBS containing 0.5 mM $MgCl_2$ and 0.1% glucose (BRET buffer). Approximately 50,000–100,000 cells/well were distributed in 96-well flat-bottomed white microplates (Greiner Bio-One). The Rluc substrate, coelenterazine-*h* (Nanolight Technologies), was dissolved in acidified alcohol at a final concentration of 5 mM and stored at −20 °C. Acidified alcohol was prepared by adding 200 μl of 3N HCl to 10 ml of ethanol. Aliquots were dissolved in BRET buffer immediately before use and added to cell suspension at a final concentration of 5 μM. BRET measurements were made using a microplate reader (POLARstar Omega, BMG Labtech) equipped with two emission photomultiplier tubes, allowing us to detect two emissions simultaneously with the highest possible resolution of 50 milliseconds for every data point. All measurements were performed at room temperature. The BRET signal is determined by calculating the ration of the light emitted by Gβ1γ2-Venus (535 nm) over the light emitted by masGRK3ct-Rluc8 (475 nm). The average base-line value (basal R) recorded prior to agonist stimulation was subtracted from BRET signal values, and the resulting difference (ΔR) was normalized against the maximal ΔR value (Rmax) recorded upon agonist stimulation. The rate constants ($1/\tau$) of the activation and deactivation phases were obtained by fitting a single exponential curve to the traces. k_{GAP} rate constants were determined by subtracting the basal deactivation rate (k_{app}) from the deactivation rate measured in the presence of exogenous RGS protein. Obtained k_{GAP} rate constants were used to quantify GAP activity.

Western Blotting—For each sample, ~5,000,000 cells were lysed in 500 μl of sample buffer (125 mM Tris (pH 6.8), 4 M urea, 4% SDS, 10% 2-mercaptoethanol, 20% glycerol, 0.16 mg/ml bromphenol blue). Western blot analysis of proteins was performed following SDS-PAGE. Blots were blocked with 5% skim milk in PBS containing 0.1% Tween 20 (PBST) for 30 min at room temperature, followed by a 90-min incubation with specific antibodies diluted in PBST containing 1% skim milk. Blots were washed in PBST and incubated for 45 min with a 1:10,000 dilution of secondary antibodies conjugated with horseradish peroxidase in PBST containing 1% skim milk. Proteins were visualized on x-ray film by SuperSignal West Femto substrate (Pierce). Band densities were quantified using ImageJ software by measuring the integrated intensity. The relative expression level of RGS proteins was determined by subtracting the background densities in the absence of exogenous RGS proteins and normalizing the resulting value as a fraction of the brightest band intensity expressing the maximal amount of RGS protein.

RGS-Gα Pull-down Assay—Mouse brain membranes (1 mg protein) in 0.5 ml of binding buffer (20 mM HEPES (pH = 8.0), 380 mM NaCl, 5 mM $MgCl_2$, 2 mM β-mercaptoethanol, protease inhibitors) containing GDP (10 μM) and AlF_4^- (20 μM $AlCl_3$ plus 10 mM NaF) were incubated for 1 h at room temperature with His-tagged RGS proteins (10 μg). Membranes were solubilized with 1% Nonidet P-40 for 1 h of incubation on ice and centrifuged at 20,000 × *g* for 1 h at 4 °C. The detergent-soluble extracts were incubated with nickel-nitrilotriacetic acid beads for 30 min at 4 °C, washed five times with wash buffer (20 mM HEPES (pH 8.0), 380 mM NaCl, 5 mM $MgCl_2$, 0.1% (w/v) $C_{12}E_{10}$,

20 mM imidazole, 3 mM dithiothreitol, protease inhibitors, 10 μM GDP and AlF_4^- (20 μM $AlCl_3$ plus 10 mM NaF) and eluted with SDS sample buffer.

CRE-Luciferase Reporter Gene Assays—HEK293T/17 cells were transfected with CRE-luc2P reporter (Promega), MOR, Gαi1, Gβ1 and Gγ2, or Gβ5 with or without R7 RGS at a 1:1:1:1:1:1:1 ratio between cDNA constructs using Lipofectamine LTX reagent in 96-well plate. 16 h after transfection, cells were treated with 50 nM isoproterenol together with serial doses of morphine for 5 h. The level of expressed luciferase were determined using a Bright-Glo luciferase assay kit (Promega) according to the instructions of the manufacturer.

Statistical Analysis—Linear regression was used to relate the k_{GAP} value to the expression level of RGS7 or RGS9-2 proteins. To compare the activities of the RGS proteins on Go *versus* Gi (Fig. 5) and their activities in the absence *versus* presence of R7BP (Figs. 6 and 7), the differences in the slopes of the regression lines were evaluated by calculating a *p* value (two-tailed) testing the null hypothesis that the slopes are all identical using GraphPad Prism 5. Kruskal-Wallis one-way analysis of variance on ranks followed by Tukey's post hoc test was performed to compare k_{GAP} values in Fig. 8*E* using SigmaPlot 11. IC_{50} values in Fig. 9*C* were compared by one-way analysis of variance followed by Tukey's post hoc test using SigmaPlot 11.

RESULTS

Live Cell Receptor-based Assays Allow Examination of the GAP Activity of R7 RGS Proteins in a Physiological Context—To visualize RGS action in living cells, we reconstituted HEK293T cells with GPCRs, Gα subunits, and BRET sensors (Gβγ-Venus and masGRK3ct-Rluc8, recently developed by Hollins *et al.* (25) (Fig. 1*A*)). In this assay system, activation of a GPCR by an agonist promotes the interaction of the Venus-tagged Gβγ subunits with the Rluc8-tagged masGRK3ct reporter producing the BRET signal. Conversely, application of an antagonist quenches GPCR-driven G protein activation and results in BRET signal decay. Indeed, activation of the heterologously expressed D2R by dopamine resulted in generation of the robust BRET response and the addition of the haloperidol deactivated the signal in a time-dependent manner (Fig. 1*B*). The rise and decay of the BRET signal are well described by single exponential fitting, allowing us to obtain rate constants for the activation and deactivation phases, respectively. No significant agonist-elicited response was observed when D2R or Gαo was not transfected (Fig. 1*C*), indicating that the BRET signal recorded in the system originates from the functional coupling of the exogenously expressed receptors and G proteins and not from the endogenous proteins contained in HEK293T cells.

We next performed a series of control experiments to demonstrate the utility of the assay in studying the GAP activity of the R7 RGS proteins. Because the GAP action of RGS proteins promotes heterotrimer reformation, they are expected to influence the kinetics of the deactivation phase of the response. However, the concurrent presence of GPCR in the system makes it necessary to ensure that the kinetics of the deactivation phase are determined by the RGS action and are not influenced by changes in GPCR activity. First, we transfected cells with increasing amounts of D2R construct and stimulated cells by application of a saturating concentration of dopamine (Fig. 1, *D–F*). An increase in the amount of D2R did not affect the amplitude of the response (Fig. 1*D*), suggesting an equal extent of the total G protein mobilization in the cells, but accelerated the onset kinetics consistent with the enhanced speed of G protein activation (Fig. 1*E*). Importantly, an increase in functional D2R had no effect on deactivation kinetics (Fig. 1*F*), indicating that the GPCR concentration does not influence the antagonist-induced termination of the response. Secondly, we applied different concentrations of dopamine to cells expressing a fixed amount of D2R (Fig. 1, *G–I*). We observed a typical sigmoidal dose-response curve of the response amplitude ($EC_{50} = 1.91 \times 10^{-7} \pm 1.67 \times 10^{-8}$ M), indicating that an increase in the agonist concentration results in an increase in the pool of the activated G proteins. As expected, enhanced GPCR activation also resulted in the increase in the rate of G protein activation (Fig. 1*H*). However no changes in the deactivation phase of the response were noted (Fig. 1*I*). These data indicate that the amount of active G protein also does not change the deactivation rates. Finally, we tested the effect of increasing the RGS concentration on the deactivation kinetics of D2R-Go signaling (Fig. 1, *J–L*). In contrast to the manipulations with GPCR and G protein concentration, an increase in the RGS7 concentration substantially accelerated the deactivation rates of the response (Fig. 1, *J* and *K*). In fact, within the concentration range tested, the calculated GAP activity of RGS7 showed a clear linear relationship with its expression level (Fig. 1*L*). The final set of control experiments ensured that the expression of components of the RGS complex did not affect the levels of the receptor, Gα subunits, or BRET sensors in cells (Fig. 2). We thus conclude that, under the assay conditions, GTP hydrolysis by G proteins is the rate-limiting step that dictates the deactivation phase of the response. The function of the R7 RGS proteins can thus be quantitatively analyzed by measuring the deactivation kinetics that show no sensitivity to fluctuations in GPCR and/or G protein concentration.

RGS7 and RGS9-2 Complexes Selectively Regulate the Gαi/o Subfamily in the absence or presence of R7BP—Members of the R7 RGS family have been shown previously to be selective GAPs for the Gαi/o proteins in the *in vitro* biochemical assays (26). However, their selectivity was never examined in the physiological context of living cells. Furthermore, on the basis of the genetic evidence from *Caenorhabditis elegans*, it was proposed recently that R7BP might unlock the GAP activity of the R7 RGS proteins toward other Gα subunits, *e.g.* Gαq (27). We therefore used the in-cell BRET assay to re-examine the regulation of the Gα GTPase by R7 RGS complexes in living cells. In these experiments, we chose a panel of representative GPCRs well known to activate each of the Gα subunits examined, *e.g.* D1R for Gαs, M1R for Gαq, D2R for Gαo and MOR for Gαz. Consistent with the *in vitro* studies, we found that, in cells, both RGS7/Gβ5 and RGS9-2/Gβ5 potently terminated a D2R-driven response *via* Gαo, a representative member of the Gαi/o family (Fig. 3, *A*, *D*, *E*, and *H*). However, we observed no regulation of the M1R-Gαq or D1R-Gαs response termination by either RGS7/Gβ5 (Fig. 3, *B*, *C*, and *D*) or RGS9-2/Gβ5 (*F*, *G*, and *H*). These data indicate that the RGS7/Gβ5 and RGS9-2/Gβ5 dimers are Gi/o subfamily-selective regulators in living cells.

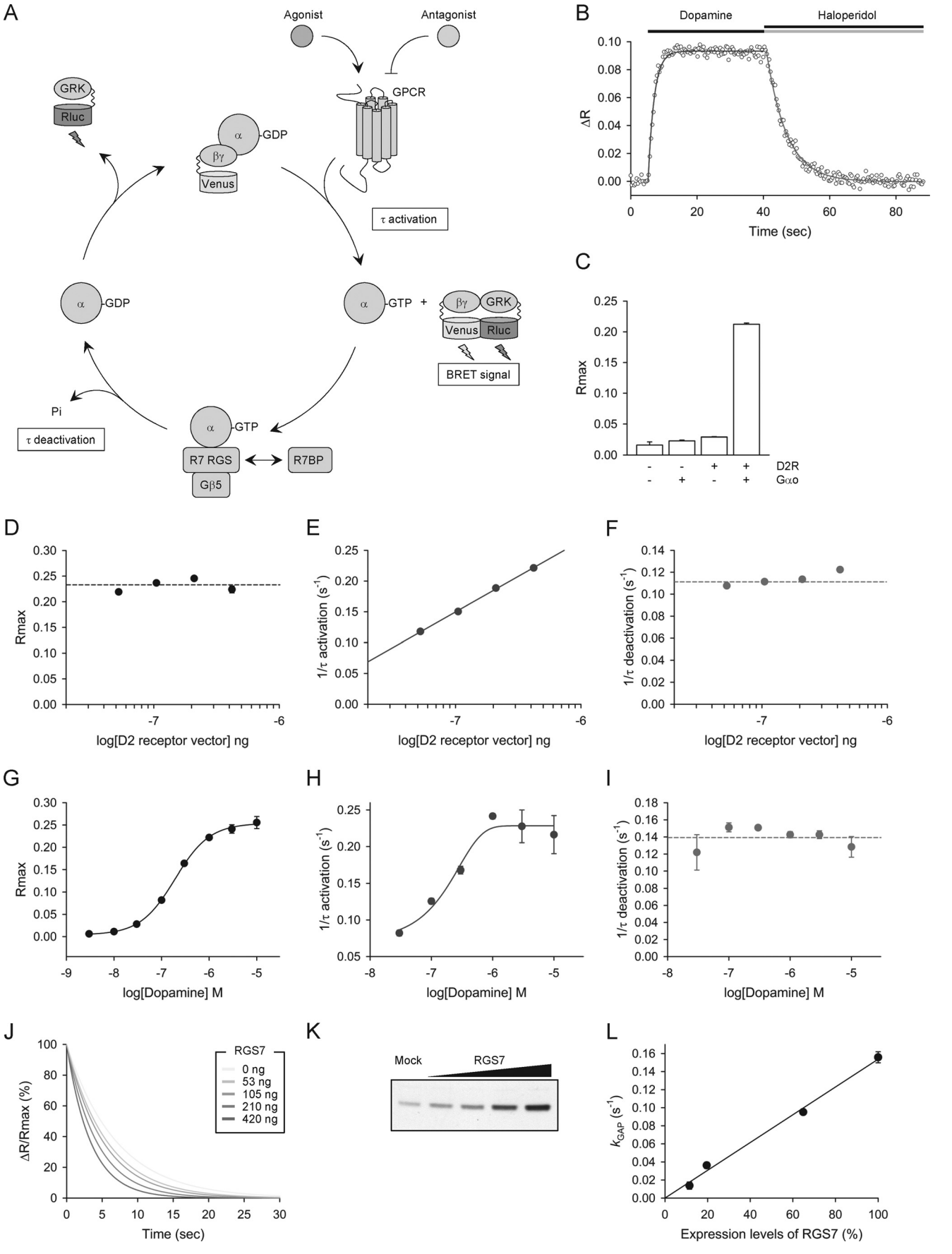
A
Agonist
Antagonist
GPCR
GRK
Rluc
α
GDP
βγ
Venus
τ activation
α
GTP
+
βγ
GRK
Venus
Rluc
BRET signal
α
GDP
Pi
τ deactivation
α
GTP
R7 RGS
R7BP
Gβ5
B
Dopamine
Haloperidol
ΔR
Time (sec)
C
Rmax
D2R
Gαo
D
Rmax
log[D2 receptor vector] ng
E
1/τ activation (s-1)
log[D2 receptor vector] ng
F
1/τ deactivation (s-1)
log[D2 receptor vector] ng
G
Rmax
log[Dopamine] M
H
1/τ activation (s-1)
log[Dopamine] M
I
1/τ deactivation (s-1)
log[Dopamine] M
J
ΔR/Rmax (%)
Time (sec)
RGS7
0 ng
53 ng
105 ng
210 ng
420 ng
K
Mock
RGS7
L
kGAP (s-1)
Expression levels of RGS7 (%)

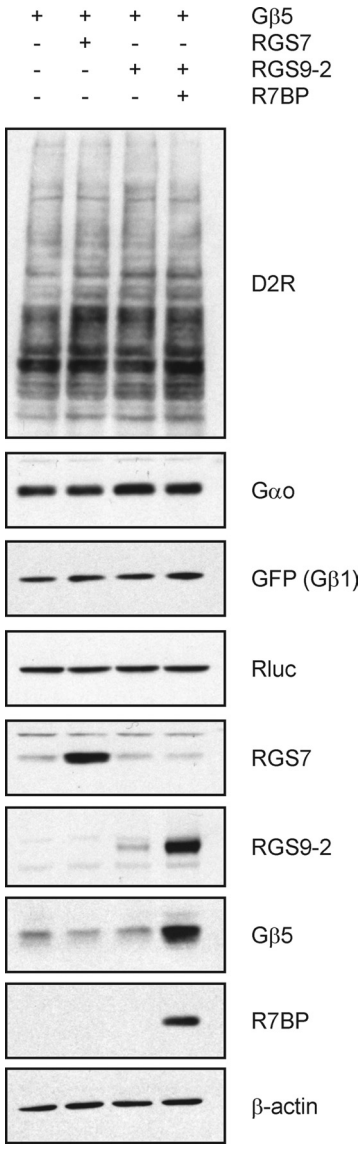

FIGURE 2. **Overexpression of the R7 RGS complex does not influence the expression levels of signaling components reconstituted in HEK293T cells.** HEK293T cells were transfected with D2R, Gαo, Venus-Gβγ, masGRK3ct-Rluc8, and Gβ5 with or without R7 RGS and R7BP. The expression levels of signaling components were analyzed by Western blotting with the indicated specific antibodies. Anti-Rluc (*Renilla* luciferase) antibody was used to detect masGRK3ct-Rluc8. Because transfection of Gβ5 without R7 RGS does not change the parameters, Rmax, and activation and deactivation rates (data not shown), Gβ5 was transfected in all conditions.

Next, we examined the possibility that R7BP may enable Gαq or Gαs regulation by RGS7 or RGS9-2 complexes. Again, we found that trimeric RGS7/Gβ5/R7BP and RGS9-2/Gβ5/R7BP complexes potently regulated Gαo deactivation but had no effect on the deactivation rates of Gαq and Gαs (Fig. 3, *I–P*). Because expression levels of RGS7 or RGS9-2 were found to be similar across cells reconstituted with various G protein subunits (data not shown), the lack of GAP activity toward Gαq and Gαs cannot be attributed to a lower expression of RGS7 and RGS9-2. Thus, we conclude that complex formation with R7BP does not influence subfamily selectivity and that the RGS7/Gβ5/R7BP and RGS9-2/Gβ5/R7BP trimers are also Gi/o subfamily-selective GAPs.

Varying G Protein Selectivity of the RGS7 and RGS9-2 Complexes within the Gαi/o Family—In addition to Gαo, the Gαi/o family contains the highly homologous proteins Gαi1-3 and the atypical subunit Gαz, which is characterized by an extremely slow intrinsic GTP hydrolysis rate (28). Because no previous studies examined the regulation of Gαz GTPase by R7 RGS proteins, we addressed this question using cell-based BRET assays. Morphine application induced a robust BRET signal from the cells reconstituted with MOR and Gαz. Consistent with biochemical measurements, Gαz responses showed very slow deactivation kinetics upon termination of signaling at MOR, with a rate constant of $3.7 \pm 0.1 \times 10^{-3}$ s^{-1}. These slow deactivation kinetics were completely unaffected by the addition of either the RGS9-2/Gβ5 or RGS7/Gβ5 complex both in the presence or absence of R7BP (Fig. 4). These observations suggest that R7 RGS complexes do not regulate Gαz signaling.

We next examined the impact of RGS9-2 and RGS7 on Gαi deactivation in comparison to Gαo. In these experiments, we titrated the amount of RGS proteins and normalized their expression levels by *post hoc* quantitative Western blotting. We used the k_{GAP} *versus* RGS concentration slope as a measure of RGS catalytic efficiency. As evident from Fig. 5*A*, RGS9-2/Gβ5 can regulate both Gαo and Gαi1 in a system containing D2R. Comparison of the two slopes indicates that RGS9-2/Gβ5 shows an ~3-fold greater preference for Gαo over Gαi1. In contrast, although RGS7/Gβ5 also effectively terminated Gαo-mediated responses, it had no detectable activity toward Gαi1 in a D2R-based system (Fig. 5*B*). We confirmed that the expression levels of Gαo and Gαi1 are similar (Fig. 5, *E* and *F*), indicating that the G protein selectivity of these two RGS proteins is not due to different levels of G protein expression. Because *in*

FIGURE 1. **Measuring GAP activity of RGS proteins by fast kinetic BRET assay.** *A*, schematic representation of the BRET assay principle. GPCR stimulation by agonist application leads to the dissociation of the G protein heterotrimer into Gβγ-Venus and GTP-bound Gα subunits. Free Gβγ-Venus interacts with masGRK3ct-Rluc8 to produce a BRET signal. Antagonist application stops production-dissociated G protein subunits by the GPCR. The Gα hydrolyzes GTP and reassociates with Gβγ-Venus, quenching the BRET signal. RGS complexes interact with GTP-bound Gα and accelerate GTP hydrolysis, speeding up heterotrimer reformation and quenching the BRET signal. *Rluc, Renilla* luciferase; *Pi,* inorganic phosphate; *GRK,* G protein-coupled receptor kinase. *B–L*, temporal and steady-state properties of reconstituted D2R-Go signaling in HEK293T cells. *B*, representative traces of changes in the BRET signal over time in a system containing the D2 dopamine receptor and Gαo ($n = 4$). Responses to sequential application of dopamine (1 μM) and haloperidol (100 μM) were recorded. *Blue* and *red trace lines* represent fitting of the activation and deactivation phases with single exponential functions, respectively. *C*, maximal responses (Rmax), elicited by saturating dopamine concentration (10 μM), are plotted for four different transfection conditions ($n = 3–6$). *D–F*, effect of increasing the amount of D2R construct on maximal response (*D*) ($n = 3$), activation (*E*) ($n = 3$), and deactivation kinetics (*F*) ($n = 3$). Separate groups of cells transfected with different amount of D2R were tested in parallel. *G–I*, effects of an increase in dopamine concentration on maximal response (*G*) ($n = 3$), activation (*H*) ($n = 3$), and deactivation kinetics (*I*) ($n = 3$). *J–L*, effect of an increase in RGS7 concentration on Go deactivation kinetics. *J*, cells were transfected with varying amounts of RGS7 construct and tested in parallel. *Trace lines* represent the exponential fit of the decay at the indicated amounts of RGS7 used for the transfection ($n = 4$). *K*, the expression levels of RGS7 in cells used in *J* were examined by Western blotting with an RGS7-specific antibody. *L*, the deactivation rate constant measured in the absence of RGS7 (0.1427 ± 0.0028 s) was subtracted from values measured in the presence of RGS7, and the resulting k_{GAP} parameters were plotted against the expression level of RGS7 measured in *K* ($n = 4$).

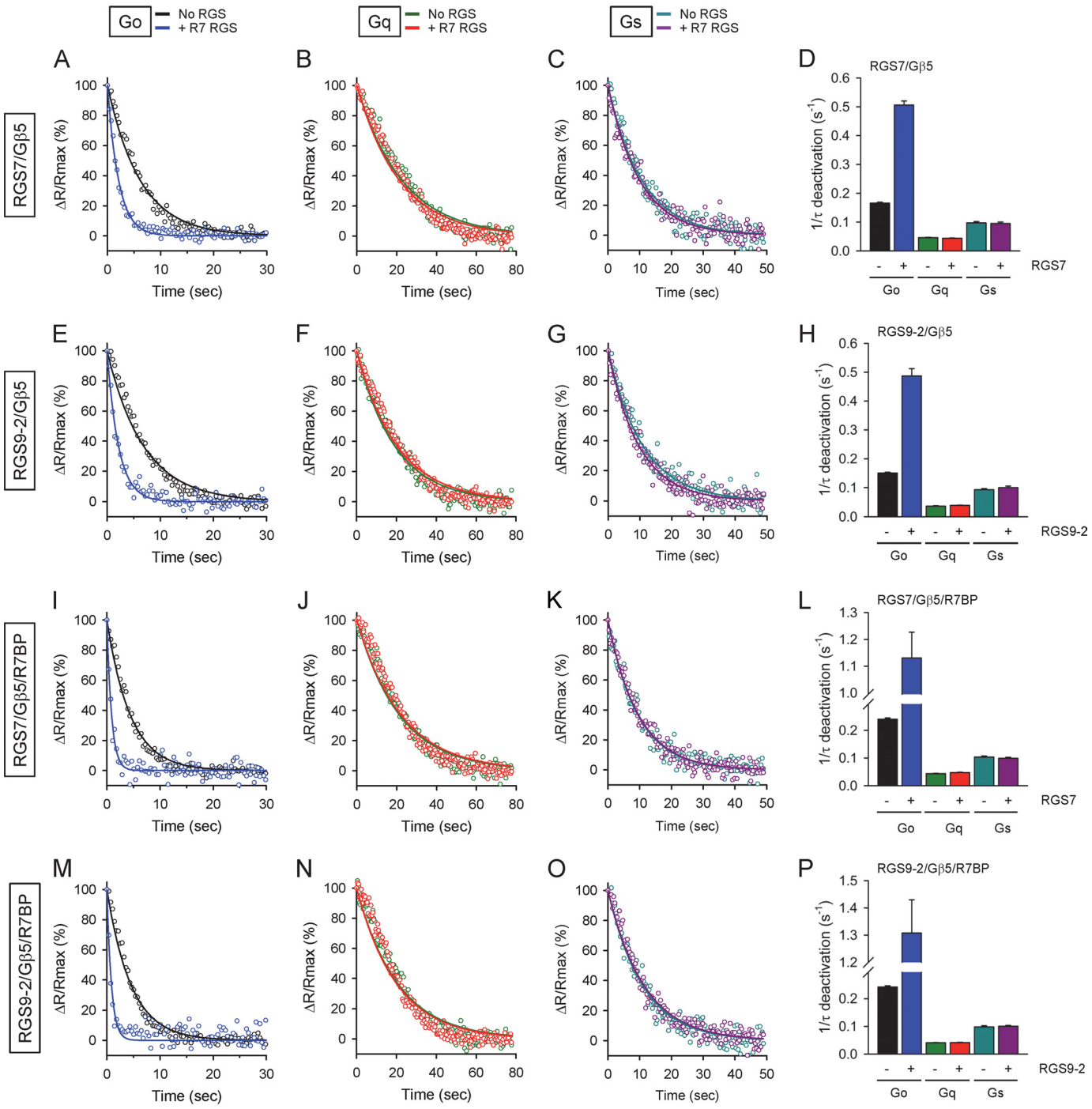

FIGURE 3. **Selectivity of RGS7 and RGS9-2 complexes across major Gα families.** D2R-Go, M1R-Gq, or D1R-Gs pairs were reconstituted in HEK293T cells by transient transfection as described under "Experimental Procedures." Cells were pretreated with the following agonists: 1 μM dopamine (for D2R), 1 μM acetylcholine (for M1R), and 10 μM dopamine (for D1R) for 35 s, followed by the application of the following antagonists: haloperidol (for D1R and D2R) and atropine (for M1R) at 100 μM. *Trace lines* represent the exponential fit of the deactivation phase. Individual combinations of receptor-Gα subunits are color-coded for the traces (*A–C*, *E–G*, *I–K*, and *M–O*) and their fittings as well as in the *bar graphs* that represent the deactivation time constants (*D*, *H*, *L*, and *P*). Four replicate samples were used for obtaining each trace.

vivo R7 RGS proteins also regulate MOR signaling, we next tested the possible effect of GPCR on Gα selectivity of RGS proteins. As with D2R signaling, RGS9-2/Gβ5 exerted a more efficacious GAP activity toward Gαo relative to Gαi1 (3-fold) (Fig. 5*C*). Again, RGS7/Gβ5 selectively regulated Gαo but not Gαi signaling when MOR was used instead of D2R to drive the responses (Fig. 5*D*). These data indicate that the RGS9-2/Gβ5 dimer is a GAP for both Gαo and Gαi, with a preference toward Gαo, that the RGS7/Gβ5 dimer is strictly selective for Gαo and does not regulate Gαi, and that G protein selectivity of these RGS proteins does not depend on the GPCR.

R7BP Potentiates the GAP Activity of RGS7 and RGS9-2 and Enables the Regulation of Gαi by RGS7 with Both D2R and MOR—We examined the effects of R7BP on the activity of RGS7 and RGS9-2 by comparing their GAP activity toward

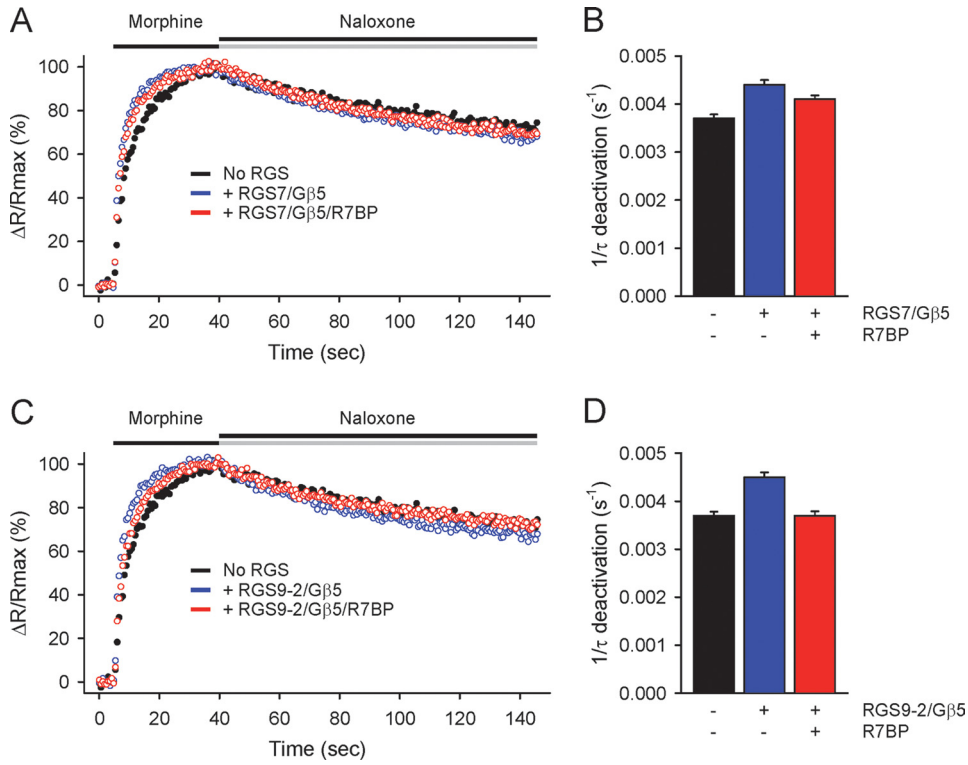

FIGURE 4. **RGS7 and RGS9-2 complexes do not regulate Gz signaling.** Gαz was activated by MOR in HEK293T cells. *A* and *C*, representative traces of changes in BRET signal upon sequential application of the MOR agonist (10 μM morphine) and antagonist (200 μM naloxone) in the absence or presence of the indicated R7 RGS proteins with and without R7BP. *B* and *D*, deactivation time constants obtained from the exponential fit of the inactivation phase of the response. Six replicate samples were used for obtaining each trace.

Gαo and Gαi1 in the D2R receptor system. Coexpression with R7BP potentiated the GAP activity of both RGS7 and RGS9-2 for Gαo. The extent of the regulation was similar and reached ~2-fold (Fig. 6, *A* and *B*). This increase in activity was independent from the regulation of the RGS9-2 expression levels by R7BP because calculated k_{GAP} values were normalized to the relative expression levels of the proteins. A similar stimulatory effect of R7BP (2.5-fold) was observed for RGS9-2 when Gαi was used in the assay instead of Gαo (Fig. 6*C*). Strikingly, coexpression with R7BP dramatically affected the ability of the RGS7/Gβ5 complex to regulate Gαi, essentially resulting in an all-or-nothing effect (Fig. 6*D*). Although, in the absence of R7BP, we detected no GAP activity of RGS7/Gβ5 toward Gαi1, the RGS7/Gβ5/R7BP trimer was capable of efficiently regulating Gαi inactivation, with the k_{GAP} values approaching those for the RGS9-2/Gβ5/R7BP complex.

We next tested the possible effect of GPCRs on the function of R7BP. For this purpose, we switched receptors from D2R to MOR (Fig. 7). With MOR, we observed similar effects of R7BP on GAP activity as with the cells transfected with D2R. R7BP potentiated RGS9-2 GAP activity toward Gαo and Gαi1 ~2-fold (Fig. 7, *A* and *C*). Likewise, R7BP enhanced RGS7 activity toward Gαo 2.5-fold (Fig. 7*B*) and played a permissive role in enabling the regulation of Gαi1 GTPase activity (*D*). Thus, we conclude that GPCRs do not have a significant effect on the ability of R7BP to augment the GAP activity of both RGS7 and RGS9-2.

RGS9-2 Is Less Efficacious but More Selective GAP Relative to RGS7—Next, we addressed questions pertaining to the relative efficiencies of RGS7 *versus* RGS9-2 in G protein deactivation and the possible GPCR selectivity of their effects (Fig. 8). To enable such comparisons, we obtained absolute quantitative values for the RGS activity. Direct comparison of RGS7/Gβ5 and RGS9-2/Gβ5 indicate that they accelerate deactivation rates in D2R- and MOR-based systems to a different extent (Fig. 8, *A* and *B*). The expression levels of RGS7 and RGS9-2 were quantified by Western blot analysis with purified RGS proteins as standards (Fig. 8, *C* and *D*). Given the linear relationship between RGS concentration and G protein deactivation rates, these values were used to normalize k_{GAP} values to derive the specific activity for each RGS protein in each GPCR system. The results allow direct comparisons of RGS efficiencies between MOR and D2R. As evident from such an analysis, RGS7 produced a 3- and 4.5-fold higher activity than RGS9-2 on D2R and MOR signaling, respectively (Fig. 8*E*). A more efficacious GAP activity of RGS7 is likely explained by its higher affinity toward the transition state of the Gαo, as evidenced by the pull-down assay between recombinant R7 RGS/Gβ5 complexes and native brain lysates (Fig. 8*F*). Thus, we conclude that RGS7 is a more potent GAP than RGS9-2, irrespective of the GPCR used in the assay. However, although RGS7 exerted a similar GAP activity in both the D2R and MOR systems, RGS9-2 was about 2-fold more effective in deactivating D2R relative to MOR signaling (Fig. 8*E*). Thus, RGS9-2 exhibits GPCR selectivity and preferentially regulates D2R signaling.

RGS7 and RGS9-2 Deferentially Control the Gαi-mediated Inhibition of Adenylate Cyclase Activity—To examine how the selectivity of RGS7 and RGS9-2 on G protein inhibition propagates the regulation of downstream effector signaling, we chose

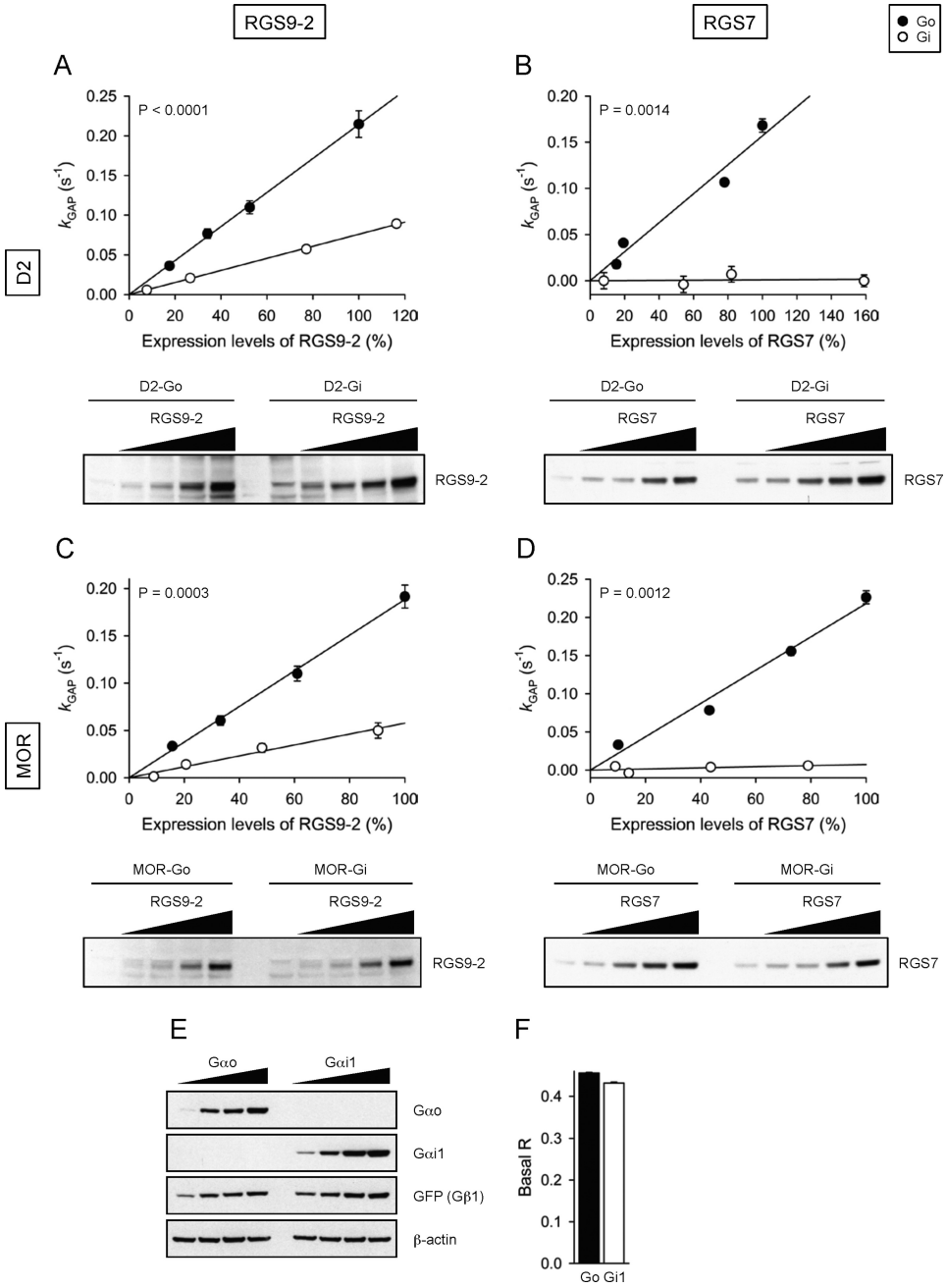

FIGURE 5. **RGS9-2/Gβ5 and RGS7/Gβ5 discriminate between Gαo and Gαi.** Gi1 (○) and Go (●) were reconstituted in HEK293T cells with D2R (*A* and *B*) or MOR (*C* and *D*). The deactivation rate constant measured in the absence of R7 RGS was subtracted from the value measured in the presence of R7 RGS, and the resulting k_{GAP} values were plotted against the expression level of R7 RGS determined by Western blotting. The slope values obtained from linear regression analysis are $2.1 \times 10^{-3} \pm 5.5 \times 10^{-5}$ for D2R-Go-RGS9-2, $7.6 \times 10^{-4} \pm 1.4 \times 10^{-5}$ for D2R-Gi-RGS9-2, $1.6 \times 10^{-3} \pm 2.2 \times 10^{-4}$ for D2R-Go-RGS7, $9.4 \times 10^{-6} \pm 5.0 \times 10^{-5}$ for D2R-Gi-RGS7, $1.9 \times 10^{-3} \pm 8.0 \times 10^{-5}$ for MOR-Go-RGS9-2, $5.8 \times 10^{-4} \pm 7.0 \times 10^{-5}$ for MOR-Gi-RGS9-2, $2.2 \times 10^{-3} \pm 2.2 \times 10^{-4}$ for MOR-Go-RGS7, and $7.4 \times 10^{-5} \pm 8.2 \times 10^{-5}$ for MOR-Gi-RGS7. Four to 12 replicate samples were used for obtaining each data point. The data shown are representative of at least two independent experiments. *E* and *F*, comparison of expression levels of transfected Go and Gi trimers. *E*, given the interdependence of Gα and Gβγ expression, we used the abundance of Venus 156–239-tagged Gβ1 to estimate the expression levels of Gαo and Gαi1. Increasing amounts of Gα subunits for transfection increase the expression levels of Gβ as expected. The conditions in the second samples from the left in experiments with Gαo and Gαi1 were used in all experiments with varying Gα subunits and show similar expression levels of Gβ. *F*, basal BRET measured before agonist application. Basal BRET reports the extent of Gα-Gβγ heterotrimer formation.

an adenylyl cyclase (AC) system for its central role in cellular signaling. AC is stimulated by Gαs and inhibited by Gαi, thus integrating G protein inputs (Fig. 9*A*). Using this system, we analyzed the effects of RGS9-2 and RGS7 on the ability of MOR to suppress cAMP production using a CRE-luciferase reporter construct. Stimulation of MOR with morphine caused a dose-dependent inhibition of β2AR-agonist isoproterenol-mediated CRE-luciferase induction (Fig. 9*B*). Cotransfection of RGS9-2 resulted in the rightward shift of the dose-response curve, increasing the IC_{50} values ~3-fold (8.38 ± 0.68 nM to 25.82 ± 2.39 nM) (Fig. 9*C*). This indicates that RGS9-2 reduces the potency of MOR-Gαi-AC signaling and is consistent with the action of RGS9-2 as a negative regulator of Gαi. In contrast, cotransfection of RGS7 did not significantly

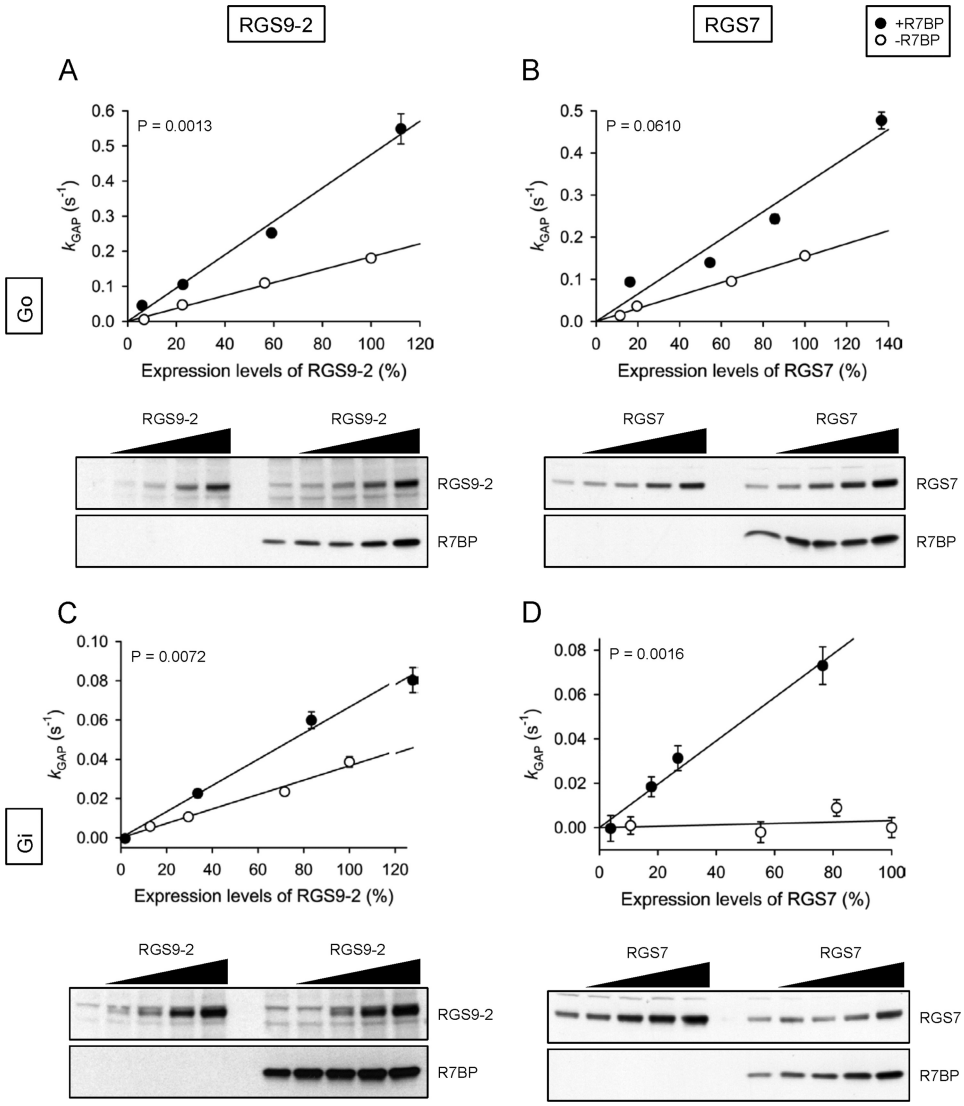

FIGURE 6. **R7BP augments the GAP activity of RGS7 and RGS9-2 toward Gαi1 and Gαo in the D2R-based system.** Gαi1 and Gαo were reconstituted in HEK293T cells with D2R, and the GAP activity of RGS7 and RGS9-2 was examined in the absence (○) or presence (●) of R7BP. Changes in the k_{GAP} values are plotted as a function of RGS concentration. Representative of two to three independent experiments yielding similar results are shown. Slope values obtained from linear regression analysis are $4.8 \times 10^{-3} \pm 3.1 \times 10^{-4}$ for D2R-Go-RGS9-2-R7BP, $1.8 \times 10^{-3} \pm 1.1 \times 10^{-4}$ for D2R-Go-RGS9-2, $3.3 \times 10^{-3} \pm 5.9 \times 10^{-4}$ for D2R-Go-RGS7-R7BP, $1.5 \times 10^{-3} \pm 8.7 \times 10^{-5}$ for D2R-Go-RGS7, $6.7 \times 10^{-4} \pm 4.2 \times 10^{-5}$ for D2R-Gi-RGS9-2-R7BP, $3.7 \times 10^{-4} \pm 3.7 \times 10^{-5}$ for D2R-Gi-RGS9-2, $9.8 \times 10^{-4} \pm 8.8 \times 10^{-5}$ for D2R-Gi-RGS7-R7BP, and $3.1 \times 10^{-5} \pm 8.5 \times 10^{-5}$ for D2R-Gi-RGS7. Four to six replicate samples were used for obtaining each data point.

affect MOR signaling to AC (Fig. 9, *B* and *C*), consistent with the lack of the RGS7 activity on Gαi revealed in the BRET assays. Thus, these data, together with data from the BRET assays, indicate that RGS proteins differentially control GPCR-mediated signaling to downstream effectors, consistent with their G protein selectivity profile.

DISCUSSION

The main result of this study is the establishment of the selectivity for two major striatal RGS proteins in their ability to regulate physiologically relevant GPCRs in the native environment of a living cell. The GAP activity of RGS proteins is usually assayed in *in vitro* systems with purified components where RGS proteins, and often only their catalytic domains, are studied in isolation from protein-protein interactions, receptors, and the membrane environment. Under those conditions, RGS proteins display very few differences in their substrate selectivity and specific activity. However, it is becoming increasingly appreciated that, *in vivo*, RGS proteins function in a tight association with other components of the GPCR signaling cascades and exist in larger macromolecular complexes (29). For example, both RGS7 and RGS9 form complexes with a range of partners that include Gβ5; the membrane anchors R7BP and R9AP (30); and the GPCRs mGlur6 (31), D2R (13, 32), MOR (33–35), m3 muscarinic (36), and GPR158/179 (37). Nevertheless, how these interactions shape RGS action in cells is poorly understood. We used a cell-based BRET assay system to study the influence of multisubunit RGS complexes on the kinetics of G protein subunit reassociation following termination of GPCR activity. We developed quantitative measures of RGS protein GAP activity in this system and applied it to investigate the

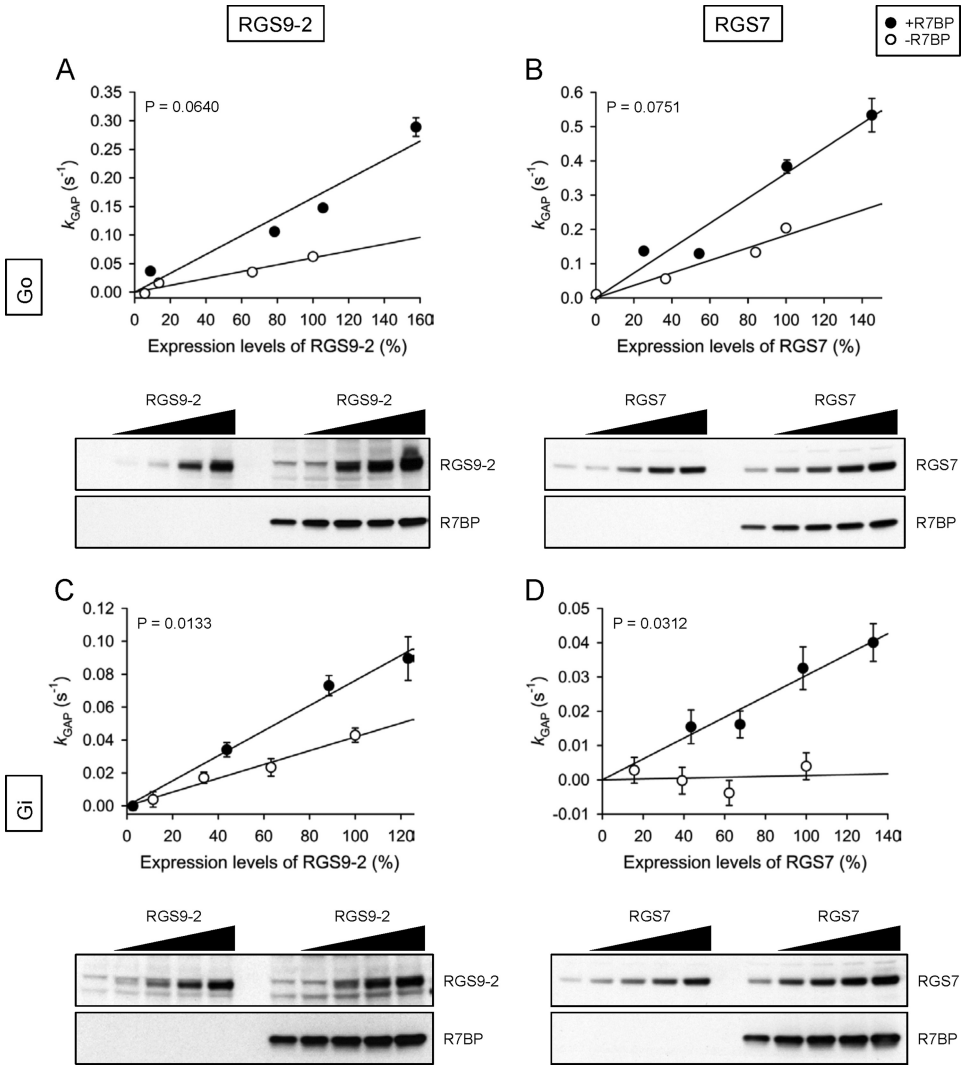

FIGURE 7. **R7BP augments the GAP activity of RGS7 and RGS9-2 toward Gαi1 and Gαo in the MOR-based system.** Gi1 and Go signaling were reconstituted in HEK293T cells with MOR, and the GAP activity of RGS7 and RGS9-2 was examined in the absence (○) or presence (●) of R7BP. Changes in the k_{GAP} values are plotted as a function of RGS concentration. Representative of two to three independent experiments yielding similar results are shown. The slope values obtained from linear regression analysis are $1.7 \times 10^{-3} \pm 3.4 \times 10^{-4}$ for MOR-Go-RGS9-2-R7BP, $6.0 \times 10^{-4} \pm 1.0 \times 10^{-4}$ for MOR-Go-RGS9-2, $3.6 \times 10^{-3} \pm 6.5 \times 10^{-4}$ for MOR-Go-RGS7-R7BP, $1.8 \times 10^{-3} \pm 2.9 \times 10^{-4}$ for MOR-Go-RGS7, $6.7 \times 10^{-4} \pm 4.2 \times 10^{-5}$ for MOR-Gi-RGS9-2-R7BP, $3.7 \times 10^{-4} \pm 3.7 \times 10^{-5}$ for MOR-Gi-RGS9-2, $3.0 \times 10^{-4} \pm 5.9 \times 10^{-5}$ for MOR-Gi-RGS7-R7BP, and $1.2 \times 10^{-5} \pm 6.8 \times 10^{-5}$ for MOR-Gi-RGS7. Four to six replicate samples were used for obtaining each data point.

activity and selectivity of the striatal RGS proteins RGS7 and RGS9-2.

The following are the key conclusions of our study (Fig. 10). First, we show that in the cellular environment RGS9-2/Gβ5 and RGS7/Gβ5 display a strong preference for Gαo over Gαi. These results are in overall agreement with published *in vitro* data (26, 38). The RGS7 complex showed the greatest selectivity for Gαo and was completely unable to inactivate Gαi in the absence of R7BP. Second, we demonstrate that the GAP activity of the RGS9-2/Gβ5 complex shows a receptor preference for D2R over MOR in regulation of the Gαo deactivation. To our knowledge, this is the first clear example of GPCR selectivity of the R7 RGS action. Although the mechanisms behind this receptor preference of the RGS9-2 complex need to be established, we speculate that they are likely determined by selective interactions of RGS9-2 with the receptors, as suggested from the studies on RGS4, that selectively interacted with the δ-opioid receptor over the μ-opioid receptor (39). Interestingly, no receptor preference was revealed for the RGS7/Gβ5 action. Third, we found that R7BP acted universally to potentiate the action of both RGS7 and RGS9-2 on both Gαi and Gαo and with both D2R and MOR. It had the most pronounced all-or-nothing effect on the ability of RGS7 to regulate Gαi, essentially switching it on. Although the design of our study did not allow distinguishing between allosteric effects and the general effects of positioning RGS complexes on the plasma membrane, we think that both mechanisms are likely involved in the action of R7BP, as exemplified in the studies on related membrane anchor R9AP (24, 41). Finally, we report that in living cells, RGS7 shows a much more potent activity relative to the RGS9-2 complex. In contrast, previous *in vitro* observations with purified proteins reported approximately equal catalytic activities of these two proteins (26). This illustrates the importance of considering a native, physiologically relevant

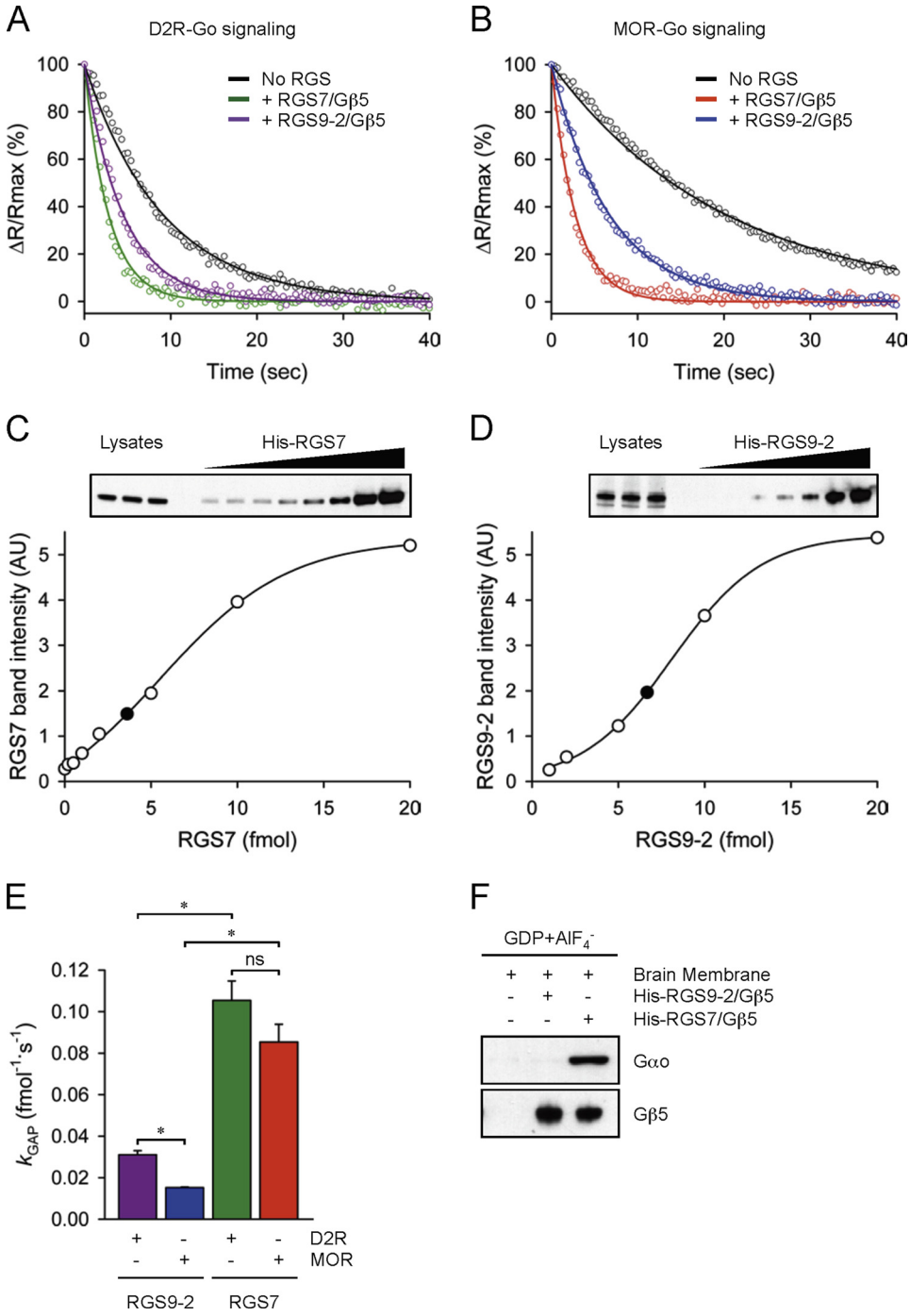

FIGURE 8. **Comparison of catalytic activities and receptor preferences of RGS7 and RGS9-2 complexes.** *A* and *B*, D2R (*A*) and MOR (*B*) signaling was reconstituted in HEK293T cells with Go, and the GAP activity of the RGS7/Gβ5 and RGS9-2/Gβ5 dimers were examined. *Trace lines* represent the exponential fit of the deactivation phase. *C* and *D*, the protein levels of RGS7 (*C*) and RGS9-2 (*D*) in the transfected cells used for the BRET assay were determined by Western blotting. Band intensities (○) obtained from recombinant proteins were used to generate a standard curve. Band intensities (1.49 ± 0.05 for RGS7 and 1.97 ± 0.08 for RGS9-2) from the triplicate samples in question were plotted on the calibration curve (○) and used to determine the amount of RGS7 and RGS9-2. *E*, the k_{GAP} values obtained from the BRET assay were divided by the amount of RGS proteins determined by Western blot analysis to compare the activity of RGS7 and RGS9-2. Six replicate samples were used for each experiment. The experiment was performed independently three times, and all showed similar results. *Error bars* represent mean ± S.E. *, $p < 0.05$, Kruskal-Wallis one-way analysis of variance on ranks followed by Tukey's post hoc test; *ns*, not significant. *F*, purified His-tagged RGS7/Gβ5 and RGS9-2/Gβ5 were incubated with mouse brain membrane fractions treated with GDP and AlF_4^-. After detergent treatment, complexes containing His-tagged proteins were purified with nickel-nitrilotriacetic acid chromatography and analyzed by Western blot analysis with Gαo and Gβ5 antibodies.

cellular environment when comparing the activities of complex RGS proteins.

It is interesting to consider the observed differences in selectivity and activity of RGS complexes in the context of striatal G protein signaling regulation. We have reported recently that changes in neuronal excitability and oxygenation trigger a remodeling of RGS complexes in the striatum (40). During this remodeling, RGS9-2 undergoes degradation, and vacated R7BP

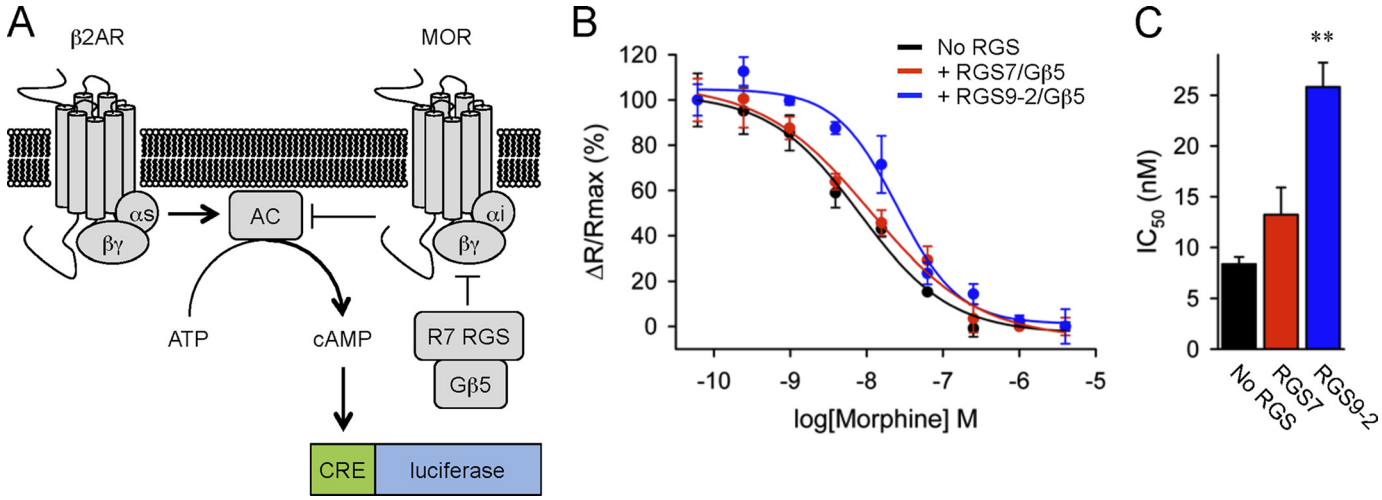

FIGURE 9. **Differential effects of RGS7 and RGS9-2 on Gαi-mediated inhibition of adenylate cyclase activity.** *A*, schematic cross-talk signaling pathway of endogenous β2-adrenergic receptor (*β2AR*) and MOR to the firefly luciferase gene regulated by the CRE response element. *B*, HEK293T cells were transfected with CRE-luc2P reporter, MOR, Gαi1, Gβ1, Gγ2, and Gβ5 with or without R7 RGS. After 5 h of treatment with 50 nM isoproterenol (*ISO*) together with serial doses of morphine, luciferase activity was measured. The highest dose of morphine treatment of cells transfected without RGS or with RGS7 or RGS9-2 inhibited ISO-induced luminescence by 68. 5 ± 1.3%, 62.9 ± 2.5%, and 61.2 ± 4.7% (S.E., $n = 4$), respectively. The average luminance at the highest dose of morphine treatment was subtracted as background, and the resulting difference (ΔR) was normalized against the maximal value upon stimulation by ISO only (Rmax). *C*, IC_{50} values were obtained by fitting a four-parameter logistic curve to the inhibition data using GraphPad Prism 5. **, $p < 0.01$, one-way analysis of variance followed by Tukey's post hoc test.

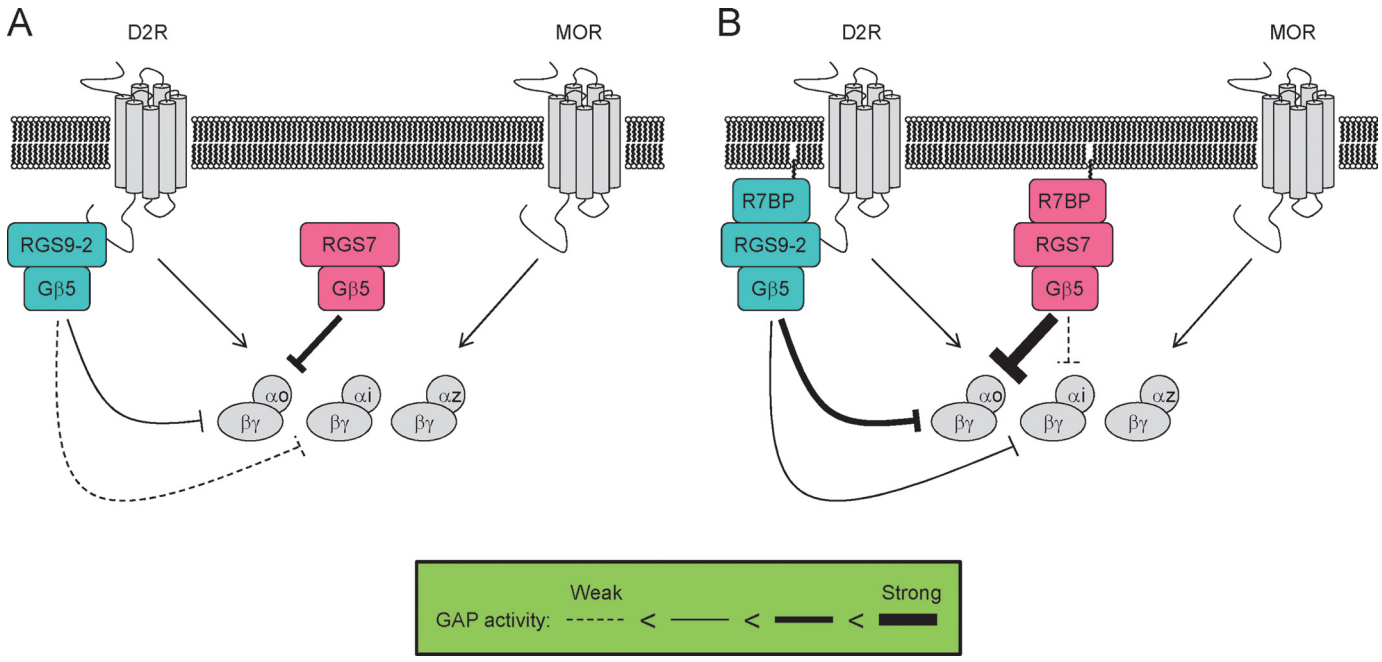

FIGURE 10. **A model for GPCR and G protein selectivity of striatal R7 RGS complexes.** RGS7 and RGS9-2 differentially regulate D2R- and MOR-mediated signaling to Gαi and Gαo in the absence (*A*) or presence (*B*) of R7BP. The thickness of the *T-shaped arrows* indicates the relative strength of GAP activity observed in this study. A thicker line represents stronger activity. RGS7 is a stronger GAP than RGS9-2. RGS9-2, but not RGS7, is capable of regulating Gαi in the absence of R7BP. Both RGS9-2 and RGS7 preferentially regulate Gαo in the absence or presence of R7BP. Although RGS7 does not show a GPCR preference, RGS9-2 complexes selectively regulate D2R over MOR.

recruits RGS7 to the plasma membrane compartments. Furthermore, multiple studies demonstrated that exposure to addictive drugs (*e.g.* cocaine, morphine, amphetamine) that influence D2R and MOR signaling also changes RGS9-2 expression (9) and, thus, likely influences the composition of RGS complexes in striatal neurons. Taken together with the results of this study, these observations suggest a model where remodeling of RGS complexes is used to adjust the strength and selectivity of striatal G protein signaling. For example, an increase in dopamine and opioid signaling may be counteracted by tweaking the GAP complex (41) to substitute less efficient RGS9-2 for the stronger RGS7 catalytic subunit. Substituting a more selective GAP for a less selective one will likely also affect the relative balance of D2R *versus* MOR signaling in the striatum. It thus appears that RGS protein complexes are more than just blunt indiscriminate tools and rather contribute to the homeostatic scaling of G protein signaling in a GPCR- and G protein-selective fashion.

Acknowledgments—We thank Dr. Nevin A. Lambert (Department of Pharmacology and Toxicology, Medical College of Georgia) for the Venus 156-239-Gβ, Venus 1–155-Gγ2, and masGRK3ct-Rluc8 constructs; Dr. Itoh Hiroshi (Department of Cell Biology, Nara Institute of Science and Technology) for Gαo, Gαi1, Gαq, and Gαs (short form) in pCMV5; Dr. William Simonds (NIDDK, National Institutes of Health, Bethesda, MD) for the rabbit anti-Gβ5 and rabbit anti-R7BP antibodies; Dr. Ping-Yee Law (University of Minnesota, Minneapolis, MN) for the HA-MOR construct; Dr. Abraham Kovoor (University of Rhode Island, Kingston, RI) for the FLAG-D2R construct; and Mr. Mohammad Fallahi-Sichani for advice on statistical analyses.

REFERENCES

1. Offermanns, S. (2003) G-proteins as transducers in transmembrane signalling. *Prog. Biophys. Mol. Biol.* **83,** 101–130
2. Hollinger, S., and Hepler, J. R. (2002) Cellular regulation of RGS proteins. Modulators and integrators of G protein signaling. *Pharmacol. Rev.* **54,** 527–559
3. Ross, E. M., and Wilkie, T. M. (2000) GTPase-activating proteins for heterotrimeric G proteins. Regulators of G protein signaling (RGS) and RGS-like proteins. *Annu. Rev. Biochem.* **69,** 795– 827
4. Fredriksson, R., and Schiöth, H. B. (2005) The repertoire of G-protein-coupled receptors in fully sequenced genomes. *Mol. Pharmacol.* **67,** 1414–1425
5. Wettschureck, N., and Offermanns, S. (2005) Mammalian G proteins and their cell type specific functions. *Physiol. Rev.* **85,** 1159–1204
6. Vassilatis, D. K., Hohmann, J. G., Zeng, H., Li, F., Ranchalis, J. E., Mortrud, M. T., Brown, A., Rodriguez, S. S., Weller, J. R., Wright, A. C., Bergmann, J. E., and Gaitanaris, G. A. (2003) The G protein-coupled receptor repertoires of human and mouse. *Proc. Natl. Acad. Sci. U.S.A.* **100,** 4903– 4908
7. Xie, K., and Martemyanov, K. A. (2011) Control of striatal signaling by g protein regulators. *Front. Neuroanat.* **5,** 49
8. Kreitzer, A. C. (2009) Physiology and pharmacology of striatal neurons. *Annu. Rev. Neurosci.* **32,** 127–147
9. Traynor, J. R., Terzi, D., Caldarone, B. J., and Zachariou, V. (2009) RGS9-2. Probing an intracellular modulator of behavior as a drug target. *Trends Pharmacol. Sci.* **30,** 105–111
10. Anderson, G. R., Posokhova, E., and Martemyanov, K. A. (2009) The R7 RGS protein family. Multi-subunit regulators of neuronal G protein signaling. *Cell Biochem. Biophys.* **54,** 33– 46
11. Cabrera-Vera, T. M., Hernandez, S., Earls, L. R., Medkova, M., Sundgren-Andersson, A. K., Surmeier, D. J., and Hamm, H. E. (2004) RGS9-2 modulates D2 dopamine receptor-mediated Ca^{2+} channel inhibition in rat striatal cholinergic interneurons. *Proc. Natl. Acad. Sci. U.S.A.* **101,** 16339–16344
12. Gold, S. J., Hoang, C. V., Potts, B. W., Porras, G., Pioli, E., Kim, K. W., Nadjar, A., Qin, C., LaHoste, G. J., Li, Q., Bioulac, B. H., Waugh, J. L., Gurevich, E., Neve, R. L., and Bezard, E. (2007) RGS9-2 negatively modulates L-3,4-dihydroxyphenylalanine-induced dyskinesia in experimental Parkinson's disease. *J. Neurosci.* **27,** 14338–14348
13. Kovoor, A., Seyffarth, P., Ebert, J., Barghshoon, S., Chen, C. K., Schwarz, S., Axelrod, J. D., Cheyette, B. N., Simon, M. I., Lester, H. A., and Schwarz, J. (2005) D2 dopamine receptors colocalize regulator of G-protein signaling 9-2 (RGS9-2) via the RGS9 DEP domain, and RGS9 knock-out mice develop dyskinesias associated with dopamine pathways. *J. Neurosci.* **25,** 2157–2165
14. Rahman, Z., Schwarz, J., Gold, S. J., Zachariou, V., Wein, M. N., Choi, K. H., Kovoor, A., Chen, C. K., DiLeone, R. J., Schwarz, S. C., Selley, D. E., Sim-Selley, L. J., Barrot, M., Luedtke, R. R., Self, D., Neve, R. L., Lester, H. A., Simon, M. I., and Nestler, E. J. (2003) RGS9 modulates dopamine signaling in the basal ganglia. *Neuron* **38,** 941–952
15. Zachariou, V., Georgescu, D., Sanchez, N., Rahman, Z., DiLeone, R., Berton, O., Neve, R. L., Sim-Selley, L. J., Selley, D. E., Gold, S. J., and Nestler, E. J. (2003) Essential role for RGS9 in opiate action. *PNAS* **100,** 13656–13661
16. Anderson, G. R., Cao, Y., Davidson, S., Truong, H. V., Pravetoni, M., Thomas, M. J., Wickman, K., Giesler, G. J., Jr., and Martemyanov, K. A. (2010) R7BP complexes with RGS9-2 and RGS7 in the striatum differentially control motor learning and locomotor responses to cocaine. *Neuropsychopharmacology* **35,** 1040–1050
17. Snow, B. E., Krumins, A. M., Brothers, G. M., Lee, S. F., Wall, M. A., Chung, S., Mangion, J., Arya, S., Gilman, A. G., and Siderovski, D. P. (1998) A G protein γ subunit-like domain shared between RGS11 and other RGS proteins specifies binding to Gβ5 subunits. *Proc. Natl. Acad. Sci. U.S.A.* **95,** 13307–13312
18. Cabrera, J. L., de Freitas, F., Satpaev, D. K., and Slepak, V. Z. (1998) Identification of the Gβ5-RGS7 protein complex in the retina. *Biochem. Biophys. Res. Commun.* **249,** 898–902
19. Chen, C. K., Eversole-Cire, P., Zhang, H., Mancino, V., Chen, Y. J., He, W., Wensel, T. G., and Simon, M. I. (2003) Instability of GGL domain-containing RGS proteins in mice lacking the G protein β-subunit Gβ5. *Proc. Natl. Acad. Sci. U.S.A.* **100,** 6604–6609
20. Martemyanov, K. A., Yoo, P. J., Skiba, N. P., and Arshavsky, V. Y. (2005) R7BP, a novel neuronal protein interacting with RGS proteins of the R7 family. *J. Biol. Chem.* **280,** 5133–5136
21. Anderson, G. R., Lujan, R., Semenov, A., Pravetoni, M., Posokhova, E. N., Song, J. H., Uversky, V., Chen, C. K., Wickman, K., and Martemyanov, K. A. (2007) Expression and localization of RGS9-2/G 5/R7BP complex *in vivo* is set by dynamic control of its constitutive degradation by cellular cysteine proteases. *J. Neurosci.* **27,** 14117–14127
22. Drenan, R. M., Doupnik, C. A., Jayaraman, M., Buchwalter, A. L., Kaltenbronn, K. M., Huettner, J. E., Linder, M. E., and Blumer, K. J. (2006) R7BP augments the function of RGS7*Gβ5 complexes by a plasma membrane-targeting mechanism. *J. Biol. Chem.* **281,** 28222–28231
23. Rojkova, A. M., Woodard, G. E., Huang, T. C., Combs, C. A., Zhang, J. H., and Simonds, W. F. (2003) Gγ subunit-selective G protein β 5 mutant defines regulators of G protein signaling protein binding requirement for nuclear localization. *J. Biol. Chem.* **278,** 12507–12512
24. Masuho, I., Celver, J., Kovoor, A., and Martemyanov, K. A. (2010) Membrane anchor R9AP potentiates GTPase-accelerating protein activity of RGS11 x Gβ5 complex and accelerates inactivation of the mGluR6-G(o) signaling. *J. Biol. Chem.* **285,** 4781–4787
25. Hollins, B., Kuravi, S., Digby, G. J., and Lambert, N. A. (2009) The c-terminus of GRK3 indicates rapid dissociation of G protein heterotrimers. *Cell. Signal.* **21,** 1015–1021
26. Hooks, S. B., Waldo, G. L., Corbitt, J., Bodor, E. T., Krumins, A. M., and Harden, T. K. (2003) RGS6, RGS7, RGS9, and RGS11 stimulate GTPase activity of Gi family G-proteins with differential selectivity and maximal activity. *J. Biol. Chem.* **278,** 10087–10093
27. Porter, M. Y., and Koelle, M. R. (2010) RSBP-1 is a membrane-targeting subunit required by the Gα(q)-specific but not the Gα(o)-specific R7 regulator of G protein signaling in *Caenorhabditis elegans*. *Mol. Biol. Cell* **21,** 232–243
28. Casey, P. J., Fong, H. K., Simon, M. I., and Gilman, A. G. (1990) Gz, a guanine nucleotide-binding protein with unique biochemical properties. *J. Biol. Chem.* **265,** 2383–2390
29. Abramow-Newerly, M., Roy, A. A., Nunn, C., and Chidiac, P. (2006) RGS proteins have a signalling complex. Interactions between RGS proteins and GPCRs, effectors, and auxiliary proteins. *Cell. Signal.* **18,** 579–591
30. Jayaraman, M., Zhou, H., Jia, L., Cain, M. D., and Blumer, K. J. (2009) R9AP and R7BP. Traffic cops for the RGS7 family in phototransduction and neuronal GPCR signaling. *Trends Pharmacol. Sci.* **30,** 17–24
31. Cao, Y., Masuho, I., Okawa, H., Xie, K., Asami, J., Kammermeier, P. J., Maddox, D. M., Furukawa, T., Inoue, T., Sampath, A. P., and Martemyanov, K. A. (2009) Retina-specific GTPase accelerator RGS11/G β 5S/R9AP is a constitutive heterotrimer selectively targeted to mGluR6 in ON-bipolar neurons. *J. Neurosci.* **29,** 9301–9313
32. Celver, J., Sharma, M., and Kovoor, A. (2010) RGS9-2 mediates specific inhibition of agonist-induced internalization of D2-dopamine receptors. *J. Neurochem.* **114,** 739–749
33. Psifogeorgou, K., Psigfogeorgou, K., Terzi, D., Papachatzaki, M. M., Varidaki, A., Ferguson, D., Gold, S. J., and Zachariou, V. (2011) A unique role of RGS9-2 in the striatum as a positive or negative regulator of opiate anal-

gesia. *J. Neurosci.* **31,** 5617–5624
34. Charlton, J. J., Allen, P. B., Psifogeorgou, K., Chakravarty, S., Gomes, I., Neve, R. L., Devi, L. A., Greengard, P., Nestler, E. J., and Zachariou, V. (2008) Multiple actions of spinophilin regulate μ opioid receptor function. *Neuron* **58,** 238–247
35. Garzón, J., López-Fando, A., and Sánchez-Blázquez, P. (2003) The R7 subfamily of RGS proteins assists tachyphylaxis and acute tolerance at μ-opioid receptors. *Neuropsychopharmacology* **28,** 1983–1990
36. Sandiford, S. L., and Slepak, V. Z. (2009) The Gβ5-RGS7 complex selectively inhibits muscarinic M3 receptor signaling via the interaction between the third intracellular loop of the receptor and the DEP domain of RGS7. *Biochemistry* **48,** 2282–2289
37. Orlandi, C., Posokhova, E., Masuho, I., Ray, T. A., Hasan, N., Gregg, R. G., and Martemyanov, K. A. (2012) GPR158/179 regulate G protein signaling by controlling localization and activity of the RGS7 complexes. *J. Cell Biol.* **197,** 711–719
38. Martemyanov, K. A., Hopp, J. A., and Arshavsky, V. Y. (2003) Specificity of G protein-RGS protein recognition is regulated by affinity adapters. *Neuron* **38,** 857–862
39. Wang, Q., Liu-Chen, L. Y., and Traynor, J. R. (2009) Differential modulation of μ- and δ-opioid receptor agonists by endogenous RGS4 protein in SH-SY5Y cells. *J. Biol. Chem.* **284,** 18357–18367
40. Anderson, G. R., Lujan, R., and Martemyanov, K. A. (2009) Changes in striatal signaling induce remodeling of RGS complexes containing Gβ5 and R7BP subunits. *Mol. Cell Biol.* **29,** 3033–3044
41. Baker, S. A., Martemyanov, K. A., Shavkunov, A. S., and Arshavsky, V. Y. (2006) Kinetic mechanism of RGS9-1 potentiation by R9AP. *Biochemistry* **45,** 10690–10697